Reversible to Irreversible Flow Transition in Periodically Driven Vortices

N. Mangan,[1,2] C. Reichhardt,[1] and C. J. Olson Reichhardt[1]
[1]*Theoretical Division, Los Alamos National Laboratory, Los Alamos, New Mexico 87545, USA*
[2]*Department of Physics, Clarkson University, Potsdam, New York 13699-5820, USA*
(Received 7 January 2008; published 5 May 2008)

We show that periodically driven superconducting vortices in the presence of quenched disorder exhibit a transition from reversible to irreversible flow under increasing vortex density or cycle period. This type of behavior has recently been observed for periodically sheared colloidal suspensions and we demonstrate that driven vortex systems exhibit remarkably similar behavior. We also provide evidence that the onset of irreversible behavior is a dynamical phase transition.

DOI: 10.1103/PhysRevLett.100.187002 PACS numbers: 74.25.Qt, 05.70.Ln

Recent experiments on periodic shearing of colloidal suspensions in a viscous media where thermal effects are negligible have shown a transition from reversible behavior to an irreversible motion as a function of increasing particle density [1,2]. The reversible and irreversible regimes were identified by measuring the net displacement of the colloids after each cycle of a periodic shear. In the reversible regime, the colloids return to their initial position at the end of each cycle, while in the irreversible regime, the colloids do not return to their starting point. A stroboscopic measurement of the displacements in the irreversible regime reveals that the colloids undergo an anisotropic random walk, with larger displacements in the shear direction. For a given colloid density, there is a threshold for the transition from reversible to irreversible behavior as a function of the strain amplitude or the distance the particles are sheared per cycle. The strain threshold decreases as the colloid concentration increases, indicating that colloid-colloid interactions play an important role in the transition. More recent modeling of this system has provided evidence that the reversible to irreversible transition is a nonequilibrium phase transition with power law divergences near the transition [3]. Other experiments on dilute sheared colloidal suspensions also indicate the importance of the particle interactions in producing irreversible or chaotic flow behaviors [4].

In this work, we consider whether the general features of the reversible and irreversible behaviors observed in the sheared colloidal system can be realized in a wider class of nonequilibrium many-particle systems. Driven particles moving over random quenched disorder provide an ideal class of systems for studying this issue [5]. Physical realizations of such systems include vortices in type-II superconductors [6,7], driven Wigner crystals [8], magnetic bubble arrays [9], driven pattern forming systems [10], and colloids moving over random landscapes [11]. In the presence of strong quenched disorder, plastic flow regimes occur in these systems even in the absence of any thermal effects. In the case of vortices, it has been established that transitions from plastic flow to smectic or elastic flow states can be induced as a function of increasing dc driving force [6]. It is not known whether there could also be a reversible to irreversible flow transition in the presence of some form of periodic forcing.

To address this question, we examine the specific system of vortices interacting with random quenched disorder, and measure vortex displacements after successive cycles of a periodic drive. Vortex lattices have been used extensively as a general system in which to understand various nonequilibrium many-body effects since numerous simulations and experiments can be performed readily over a wide range of parameters. It has been shown that many of the nonequilibrium effects observed in the vortex system also occur in other systems such as driven colloidal assemblies [11,12]; thus, we expect that our results will be generic to other driven interacting point particle systems with quenched disorder.

The simulation system consists of a two-dimensional sample of size $L \times L$ with periodic boundary conditions in the x and y directions. The sample contains N_v vortices at a vortex density of $n_v = N_v/L^2$. The vortex-vortex interaction force is $\mathbf{F}_i^{vv} = \sum_{i \neq j}^{N_v} f_0 K_1(R_{ij}/\lambda)\hat{\mathbf{R}}_{ij}$, where K_1 is a modified Bessel function, $R_{ij} = |\mathbf{R}_i - \mathbf{R}_j|$ is the distance between vortex i and j located at $\mathbf{R}_i$ and $\mathbf{R}_j$, $\hat{\mathbf{R}}_{ij} = (\mathbf{R}_i - \mathbf{R}_j)/R_{ij}$, $f_0 = \phi_0/(2\pi\mu_0\lambda^3)$, λ is the London penetration depth, and $\phi = h/2e$ is the flux quantum. Lengths are measured in units of λ and the sample size is $L = 64\lambda$. For $R_{ij} > \lambda$ the vortex interaction falls off rapidly, so a finite cutoff on the interaction range is placed at $R_{ij} = 6\lambda$. The quenched disorder is modeled as $N_p = 100$ randomly placed parabolic pinning traps of radius $r_p = 0.3\lambda$ and strength F^p, with $\mathbf{F}_i^p = \sum_k^{N_p} F^p(R_{ik}/r_p)\Theta(r_p - R_{ik})\hat{\mathbf{R}}_{ik}$, where Θ is the Heaviside step function, $R_{ik} = |\mathbf{R}_i - \mathbf{R}_k^p|$, $\hat{\mathbf{R}}_{ik} = (\mathbf{R}_i - \mathbf{R}_k^p)/R_{ij}$, and $\mathbf{R}_k^p$ is the location of pin k. The periodic drive is produced by the Lorentz force from a square wave current of period τ, which we model as $\mathbf{F}^{\rm ext}(t) = F^{\rm ext}\mathrm{sgn}[\sin(2\pi t/\tau)]\hat{\mathbf{x}}$, such that a vortex under the influence of only the driving force undergoes a displacement of

$d = F^{\text{ext}}\tau/2\eta$ in half a drive cycle. In this work, except where indicated, we fix $F^{\text{ext}} = 0.8f_0$ and vary d by changing τ. The overdamped equation of motion for a single vortex i is

$$\eta \frac{d\mathbf{R}_i}{dt} = \mathbf{F}_i^{vv} + \mathbf{F}_i^{p} + \mathbf{F}^{\text{ext}}(t), \quad (1)$$

where $\eta = 1$ is the viscous damping term. The vortices are initialized in random positions. We use the same protocol as in Ref. [1] to stroboscopically determine the vortex locations after each drive cycle and extract the effective diffusivities. The mean square vortex displacement R_x^d and R_y^d in the x and y directions is measured as a function of the number n of drive cycles:

$$R_\alpha^d(n\tau) = N_v^{-1} \sum_i^{N_v} [(\mathbf{R}_i(t_0 + n\tau) - \mathbf{R}_i(t_0)) \cdot \hat{\boldsymbol{\alpha}}]^2, \quad (2)$$

where $\alpha = x, y$. From this quantity we follow Ref. [1] and define an effective diffusivity $D_\alpha = R_\alpha^d/2t$. When the behavior is reversible the vortices return to their initial positions after each drive cycle and $R_{x,y}^d$ and $D_{x,y}$ are zero. We observe an initial transient period of finite $R_{x,y}^d$, after which the system settles into a stationary state that is either reversible or irreversible. The diffusivities are measured only after this stationary state is reached. A similar transient behavior was observed in the shearing experiments of Ref. [1]. We also measure the vortex velocity in the x direction given by $V_x = N_v^{-1} \sum_i^{N_v} \mathbf{v}_i \cdot \hat{\mathbf{x}}$, where $\mathbf{v}_i$ is the velocity of vortex i. In all of our simulations, $N_v > N_p$ so that we avoid any regimes where the vortices are all pinned. For all of the parameter sets considered in this work, the vortices in the reversible regime are moving during the drive cycle.

We find a transition from reversible to irreversible behavior as a function of displacement per cycle d and vortex density n_v. In Fig. 1(a) we highlight the locations of the vortices every 0.01τ during $n = 4$ four cycles with $d = 48\lambda$ and $n_v = 0.052/\lambda^2$. Most of the vortices are moving while a small number of vortices remain pinned. In Fig. 1(b) we illustrate the same system with the vortex positions marked once per cycle during $n = 100$ cycles. Here, all of the vortices return to their initial position at the end of each cycle, so all of the points marking the position of an individual vortex coincide. This indicates that the system is undergoing a reversible flow. For increasing d there is a transition to an irreversible flow state. In Fig. 1(c) we show the stroboscopic locations of the vortices in $n = 25$ cycles for the same system as in Figs. 1(a) and 1(b) but with $d = 160\lambda$. In this case, the vortices do not return to their initial positions after each cycle. When the number of cycles increases, the vortices continue to move further from their starting point after each cycle. Figure 1(d) illustrates the anisotropic nature of the vortex displacements for the system in Fig. 1(c) during $n = 100$ cycles.

In Fig. 2(a) we plot the cumulative mean squared displacements R_x^d and R_y^d versus drive cycle number for the sample in the irreversible regime shown in Figs. 1(c) and 1(d). The dashed line fits indicate that the vortices are performing an anisotropic random walk similar to that found in the irreversible regime for the sheared colloidal system of Ref. [1]. By conducting a series of simulations in which we vary d and n_v, we can extract the effective diffusivities and determine the thresholds for the irreversible behavior.

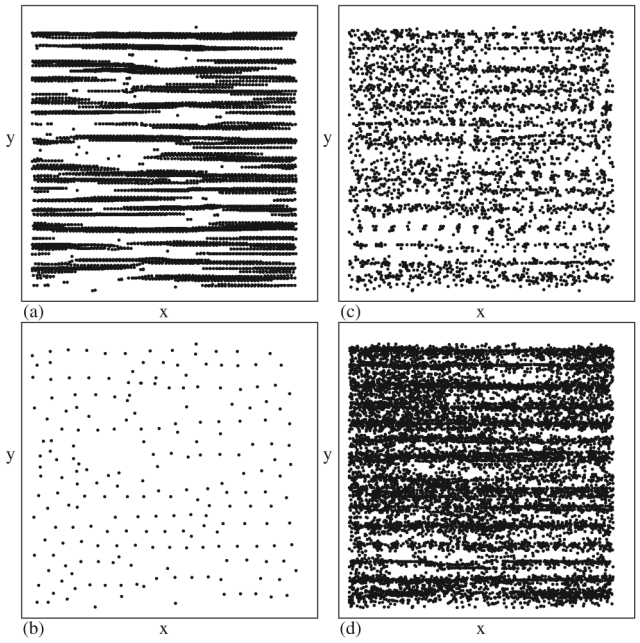

FIG. 1. Black dots: Stroboscopic vortex positions marked every 0.01τ in (a) and every τ in (b),(c),(d). (a) Vortex positions during $n = 4$ cycles in a sample with $n_v = 0.052/\lambda^2$ and $d = 48\lambda$. (b) Vortex positions in the same sample as (a). In this reversible regime, all of the vortices return to their initial positions after each cycle. (c) Positions in a sample with a longer $d = 160\lambda$ in $n = 25$ cycles. The vortices do not return to their initial positions and the behavior is irreversible. (d) The same sample as (c) for $n = 100$ cycles showing that the displacements are anisotropic.

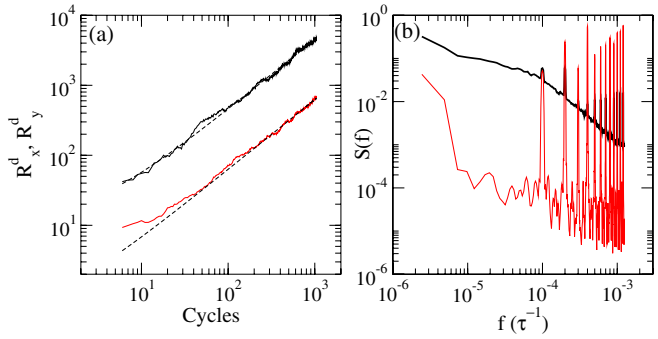

FIG. 2 (color online). (a) R_x^d (top line) and R_y^d (bottom line) versus the number of drive cycles n for the system in Figs. 1(c) and 1(d) in the irreversible regime. The particles undergo an anisotropic random walk motion. Dotted lines: fits used to obtain D_x and D_y. (b) $S(f)$ for the irreversible regime in Fig. 1(c) (top line) and the reversible regime in Fig. 1(a) (bottom line).

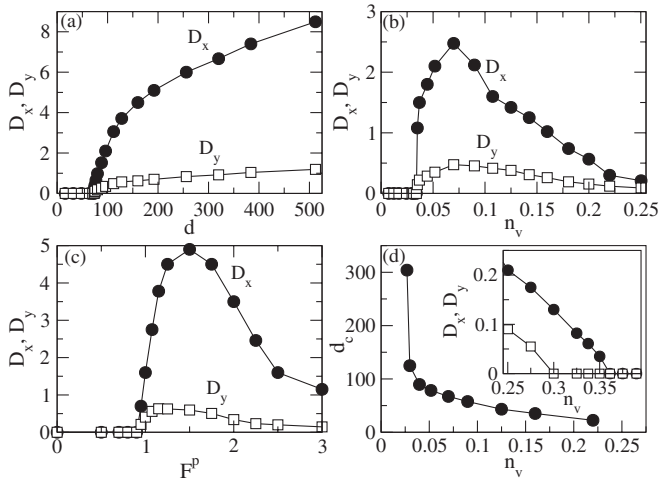

FIG. 3. Diffusivities D_x and D_y versus d for fixed $n_v = 0.052/\lambda^2$. (b) D_x and D_y versus n_v for fixed $d = 96\lambda$. (c) D_x and D_y versus F^p for fixed $n_v = 0.052/\lambda^2$ and $d = 160\lambda$. (d) Threshold displacements d_c for the transition to irreversible behavior versus n_v for fixed $F^p = 1.25f_0$. Inset: D_x (circles) and D_y (squares) at $n_v \geq 0.25/\lambda^2$ continued from (b).

In Fig. 3(a) we plot D_x and D_y versus d for a sample with fixed $n_v = 0.052/\lambda^2$. There is a clear threshold $d_c = 80\lambda$ marking the transition from reversible behavior with $D_x = D_y = 0$ to irreversible behavior with nonzero D_x and D_y. Above d_c, D_x and D_y monotonically increase with d. Figure 3(b) shows $D_{x,y}$ for fixed $d = 96\lambda$ and varied vortex density n_v. There is a threshold density $n_v = 0.034/\lambda^2$ below which the system is reversible and above which the behavior becomes irreversible. The diffusivity passes through a peak as n_v increases above the threshold, while D_x and D_y decrease at higher values of n_v when the increasing strength of the vortex-vortex interactions leads to an effective caging effect. The inset of Fig. 3(d) illustrates the appearance of two additional phases at higher n_v. For $0.3/\lambda^2 \leq n_v < 0.36/\lambda^2$, $D_y = 0$ but D_x remains finite, resulting in a smectic phase [6] where the vortices move in one-dimensional chains that are decoupled in the y direction. For $n_v \geq 0.36/\lambda^2$, the system enters a jammed phase where the vortex-vortex interactions dominate, the vortices form a rigid lattice, and the motion is reversible again.

In Fig. 3(c) we illustrate the effect of the pinning strength F^p on the dynamics for a sample with $d = 96\lambda$ and $n_v = 0.052/\lambda^2$. For weak F^p the system acts reversibly, since when $F^{\text{ext}} > F^p$, all the vortices depin and there is no local shear in the vortex lattice. In the colloidal shearing experiments of Ref. [1], the shear geometry generated a velocity differential in the system, and when the total shear was too small, the colloids moved reversibly. At high F^p, the vortices are immobilized by the pinning sites and the behavior is reversible again. Irreversible behavior occurs for intermediate values of F^p, as shown in Fig. 3(c) by the peak in D_x and D_y at $F^p \approx 1.5f_0$. In Fig. 3(d) we plot d_c, the threshold displacement per cycle required to induce irreversible behavior, versus vortex density n_v, showing that d_c decreases with increasing n_v. There is a divergence in d_c near the matching density $n_v = 0.0244/\lambda^2$ where the number of vortices equals the number of pinning sites. If $N_v < N_p$, all the vortices are pinned and the system enters a reversible state. As $N_v \rightarrow N_p$ from above, the distance between nonpinned vortices diverges and the vortices must be driven over longer distances in order to permit the nonpinned vortices to interact with each other and produce the irreversible behavior.

In general, our results are in good agreement with the shear experiments of Ref. [1], where a threshold strain which decreases with increasing colloid density must be applied to produce irreversible motion. d_c diverges as the threshold is approached from above. Our results suggest that if the colloidal experiment were performed at higher colloid density than considered in Ref. [1], the diffusivity should decrease dramatically and could drop to zero if a jamming transition occurs. It may also be possible that the colloidal motion will become banded, which would be analogous to the smectic state.

In the shear experiments the transition from reversible to irreversible behavior can be visualized directly by video microscopy [1], while for most vortex systems, direct imaging of the vortex motion is difficult. A straightforward method for probing the nature of the vortex dynamics is through voltage noise fluctuations, where the voltage is proportional to the vortex velocity. In Fig. 4(a) we plot V_x versus cycle number n for the same system shown in Figs. 1(a) and 1(b) in both the reversible and irreversible regimes. The velocities are sampled at a rate of 0.01τ. In

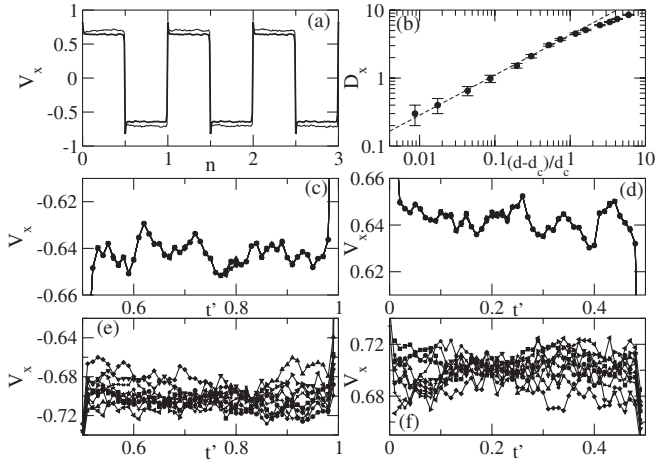

FIG. 4. (a) V_x versus cycle number n for (light line) the reversible regime in Fig. 1(a) and (heavy line) the irreversible regime in Fig. 1(c). (b) D_x from Fig. 3(a) vs $(d - d_c)/d_c$. Dashed line: logarithmic fit $D_x \propto (d - d_c)^\beta$ with $\beta = 0.59$. (c)–(f) Overlapping time traces of V_x during 10 cycles plotted versus $t' = t - t \mod \tau$. Reversible regime from Fig. 1(a): (c) lower half cycle, (d) upper half cycle. Irreversible regime from Fig. 1(c): (e) lower half cycle, (f) upper half cycle.

Fig. 4(a), we see that V_x follows the square wave of the driving force and that the average V_x for the two states is similar. We can superimpose the velocity curves in each cycle by plotting V_x versus t', where $t' = t - t \bmod \tau$, and compare the velocity fluctuations in the two regimes. In Figs. 4(c) and 4(d) we plot the superimposed fluctuations of V_x for 10 cycles in the reversible regime for the negative and positive portions of the cycle. Here, the fluctuations of V_x are nearly identical in each cycle, indicating that the vortices are flowing along the same trajectories during each cycle. In the irreversible regime, shown in Figs. 4(e) and 4(f), the velocity fluctuations differ during each cycle and the curves do not overlap. We observe a similar behavior for the fluctuations in the y direction. Since the power spectrum of the fluctuations can be measured readily in experiment [13], we compute $S(f) = |\int |V_x(t)| e^{-2\pi i f t} dt|^2$. Figure 2(b) shows that a broad spectrum appears in the irreversible regime, while in the reversible regime the noise power is much lower and strong harmonic frequencies appear. These results show that the reversible to irreversible transition can be identified through noise measurements. A more direct visualization experiment could be performed by periodically driving a two-dimensional colloid system interacting with a random substrate [12] or optical traps [14].

The colloidal shearing experiments of Refs. [1,3] found evidence of a dynamical phase transition into the irreversible state, along with an initial transient behavior of a duration that diverges near the transition. We find a similar transient behavior in our system. If we consider D_x and D_y in Fig. 2(a) as an order parameter, Fig. 4(b) shows that we find a reasonable scaling of $D_x \propto (d - d_c)^\beta$ with $\beta = 0.59$, consistent with either directed percolation in two dimensions [15] or conserved directed percolation. The latter was recently proposed as the universality class of the colloidal shear experiments [16]. It would be interesting to determine whether a similar power law divergence occurs in the average displacements near the strain threshold in the colloidal system.

In summary, we have shown with numerical simulations that a nonthermal transition from reversible to irreversible flow behavior occurs for periodically driven vortex systems in the presence of quenched disorder. The transition is characterized by performing stroboscopic measurements of the vortex locations after each drive cycle. We find that there is a threshold in the displacement per cycle above which the system acts irreversibly. In the irreversible regime, the vortices undergo an anisotropic random walk. The threshold decreases as the vortex density increases. The transition can also be identified by analyzing the voltage noise fluctuations during each cycle. Our results are remarkably similar to recent experimental observations of a transition to irreversible flow for sheared colloids. In the colloid system, the velocity dispersion created by the shearing process permits neighboring colloids to undergo different random displacements. In the vortex system, the pinning sites create velocity dispersion by generating local shear in the vortex lattice. The transition to the irreversible state is consistent with either two-dimensional directed percolation or conserved directed percolation. Our results suggest that the behavior of the colloidal shear experiments may be general to driven particle systems with quenched disorder.

We thank E. Ben-Naim, M. Hastings, and D. Pine for useful discussions. This work was carried out under the auspices of the NNSA of the U.S. DOE at LANL under Contract No. DE-AC52-06NA25396.

[1] D. J. Pine, J. P. Gollub, J. F. Brady, and A. M. Leshansky, Nature (London) **438**, 997 (2005).
[2] J. Gollub and D. Pine, Phys. Today **59**, No. 8, 8 (2006).
[3] L. Corté, P. M. Chaikin, J. P. Gollub, and D. J. Pine, Nature Phys. (to be published).
[4] J. R. Brown *et al.*, Phys. Rev. Lett. **99**, 240602 (2007).
[5] J. Watson and D. S. Fisher, Phys. Rev. B **54**, 938 (1996); **55**, 14 909 (1997).
[6] H. J. Jensen, A. Brass, and A. J. Berlinsky, Phys. Rev. Lett. **60**, 1676 (1988); M. C. Faleski, M. C. Marchetti, and A. A. Middleton, Phys. Rev. B **54**, 12427 (1996); C. J. Olson, C. Reichhardt, and F. Nori, Phys. Rev. Lett. **80**, 2197 (1998); A. B. Kolton, D. Domínguez, and N. Grønbech-Jensen, Phys. Rev. Lett. **83**, 3061 (1999).
[7] K. Moon, R. T. Scalettar, and G. T. Zimányi, Phys. Rev. Lett. **77**, 2778 (1996); L. Balents, M. C. Marchetti, and L. Radzihovsky, Phys. Rev. B **57**, 7705 (1998); P. Le Doussal and T. Giamarchi, *ibid.* **57**, 11 356 (1998).
[8] M. C. Cha and H. A. Fertig, Phys. Rev. B **50**, 14 368 (1994); C. Reichhardt and C. J. Olson Reichhardt, Phys. Rev. Lett. **93**, 176405 (2004).
[9] R. Seshadri and R. M. Westervelt, Phys. Rev. Lett. **70**, 234 (1993).
[10] A. Sengupta, S. Sengupta, and G. I. Menon, Phys. Rev. B **75**, 180201(R) (2007).
[11] C. Reichhardt and C. J. Olson, Phys. Rev. Lett. **89**, 078301 (2002).
[12] A. Pertsinidis and X. S. Ling, Phys. Rev. Lett. **100**, 028303 (2008).
[13] A. C. Marley, M. J. Higgins, and S. Bhattacharya, Phys. Rev. Lett. **74**, 3029 (1995); Y. Togawa, R. Abiru, K. Iwaya, H. Kitano, and A. Maeda, *ibid.* **85**, 3716 (2000); S. Okuma, J. Inoue, and N. Kokubo, Phys. Rev. B **76**, 172503 (2007).
[14] D. G. Grier, Nature (London) **424**, 810 (2003).
[15] K. A. Takeuchi, M. Kuroda, H. Chaté, and M. Sano, Phys. Rev. Lett. **99**, 234503 (2007); and references therein.
[16] G. I. Menon and S. Ramaswamy, arXiv:0801.3881; and references therein.